Study on Synthesis of Doped Polyaniline with Alumina and its Anticorrosion Properties as an Additive in Paint Coating

Seifi, Mohammad Hassan; Sharifzadeh Baei, Mazyar
Department of Chemical Engineering, Ayatollah Amoli Branch, Islamic Azad University, Amol, I.R. IRAN

Ghorbanib, Mohsen*+
Faculty of Chemical Engineering, Babol Noshirvani University of Technology, Shariati Ave., Babol, I.R. IRAN

Omidkhah, Mohammad Reza
Department of Chemical Engineering, Faculty of Engineering, Tarbiat Modares University, Tehran, I.R. IRAN

ABSTRACT: *In this study, polyaniline nanocomposite with aluminum oxide (PANI/Al_2O_3) was synthesized in situ polymerization method and the anti-corrosion ability of nanocomposite was investigated. Products were identified by chemical analysis of Fourier Transform InfraRed (FT-IR) spectroscopy, X-ray crystallography (XRD), and thermal weighing calorimetric analysis (TGA). Also, anti-corrosion properties were analyzed by Open Circuit Potential (OCP)analysis, Electrochemical Impedance Spectroscopy (EIS), and potentiodynamic polarization curves. To investigate anti-corrosion performance, different percentages of nanocomposites (3, 6, 9, and 12 %) were added to industrial paint and applied to steel sheets as a coating. The results of corrosion performance illustrated that the steel sheets coated with PANI/Al_2O_3 nanocomposites along with the paint, have less corrosion compared to the samples of pure steel sheets and the cases coated with PANI/Al_2O_3 nanocomposites. Also, the 6 % coating containing PANI/Al_2O_3 nanocomposite along with paint on steel sheets showed the best anti-corrosion properties. The open-circuit potential analysis results make it clear that the coatings containing PANI/Al_2O_3 nanocomposite with paint have a higher performance compared to pure paint coatings in 3 wt% NaCl solution. EIS analysis revealed resistance of the coating containing 6 % PANI/Al_2O_3 along with the paint is more than other samples in 3 % NaCl solution.*

KEYWORDS: Polyaniline; Composite; Corrosion protection; Industrial paint.

INTRODUCTION

One of the most important scientific, technical, and economic topics that have attracted the attention of some scientists and researchers for more than one hundred years, and many studies have been done on it, and subject is corrosion, especially "corrosion of metals" [1-4]. Corrosion of metals in different environments depends not only on the type of metal and alloy but also on various factors such as depth [5], temperature [6], amount and type of dissolved gases [7], amount and type of organic and inorganic compounds [8], speed of movement and biological factors of the environment [9, 10]. The most comprehensive definition of corrosion is the destruction of materials by environmental reaction[11].

*To whom correspondence should be addressed.
+ E-mail: m.ghorbani@nit.ac.ir
1021-9986/2023/10/3257-3266 10/$/6.00

Corrosion can be combated in various ways, such as controlling the electrode potential so that the metal becomes immune or ineffective [12, 13], such as applying cathodic or anodic protection [11, 14, 15], reducing corrosion rate by adding corrosion inhibitors to the environment, and applying a polymer coating [16, 17]. In recent years, many ways of corrosion protection have been used, among which protection through a conductive and stable organic coating synthesized by chemical and electrochemical methods [18-20] have been noticed more. Some useful applications of conductive polymers include corrosion protection [21, 22], rechargeable batteries [23], sensorss [24], optical power tools [22], and light emitting devices [25]. Among the types of conductive polymers used as corrosion protectors, polyaniline (PANI) is the most widely used. PANI has also attracted special attention due to its features such as easy synthesis, low cost, wide application and high polymerization efficiency [26]. The structure of polyaniline consists of recurrent phenylenediamine groups and quinoid imine groups [27]. Given that the corrosion potential due to the presence of the polymer coating shifts to positive values, it seems that polyaniline provides anodic protection. Polyaniline can also prevent the penetration of invasive species by forming a barrier-like protective layer, thereby reducing the corrosion rate of the metal [28].

In recent years, the application of nanoparticles in the synthesis of PANI and the preparation of nanocomposites and the subsequent function of these nanocomposites in paints and epoxy-resins have been further examined and the corrosion behavior of coatings applied on steel has been investigated [29]. Among the nanoparticles used in the preparation of PANI nanocomposites, nanoparticles of zinc oxide [30], titanium oxide [31] and carbon nanotubes [32] can be mentioned. Studies on coatings containing PANI nanocomposites /carbon nanotubes have shown that the nanocomposites used in the applied coatings have improved the corrosion protection of the steel by reinforcing the passive layer formed on the steel. On the other hand, studies on coatings containing PANI/ZnO nanocomposites have shown that nanocomposites increase the corrosion resistance of steel.

So far, much research has been done on the corrosion of metals by PANI nanocomposites. For example, new PANI-TiN nanocomposites and PANI-TiN/epoxy coatings with increased corrosion resistance based on the synergistic effect of TiN nanoparticles and PANI nanoparticles were obtained by *Situ et al*. [33]. According to the results, the composite with 4% by weight has achieved more favorable results. According to another study by *Park et al*. [34], polyaniline composites and carbon nanotubes have been synthesized to investigate corrosion properties and electrical conductivity. According to this study, PANI-CNT composite has the highest anti-corrosion performance of the respective epoxy coating. In addition, corrosion resistance increased with immersion time. In the previous researches, paint is prepared from the synthesis of nanocomposite with epoxy. But in this research, nanocomposite is used as a pigment to improve anti-corrosion properties in industrial paints. In this study, by strengthening the structure of the protective coating, an attempt was made to significantly improve the protective properties compared to the previous types by using the composite as a coating in combination with industrial painting color with corrosion-resistant ability. The reason for this advantage is the use of alumina due to those excellent properties in this composite, improving the properties of PANI as a bed polymer, causing more and more favorable resistance to the penetration of interfering ions and oxygen and water molecules to the protective coating and then to the metal surface. Present work opens new window to use a new, low-cost and easy method to synthesize nanomaterials pigments as well as great anticorrosion behavior. Herein, the synthesis of (PANI/Al_2O_3) composite was performed through the polymerization pathway and Al_2O_3 doping. Al_2O_3 acts as a doping operator that the obtained integrated PANI/Al_2O_3 composite are blended into the paint. At long last, this paint is utilized as a coating for steel surface and examined anti-corrosion and self-healing performance against 3% of the NaCl solution.

EXPERIMENTAL SECTION

Materials

Aniline monomer ($C_6H_5NH_2$), ammonium peroxydisulfate ($(NH_4)_2S_2O_8$), Alumina (Al_2O_3) nanoparticles, hydrochloric acid (HCl), methanol (CH_3OH) and acetone (C_3H_6O) were purchased from Merck Co. The commercial paint was purchased from Aria Pars Company. The steel sheets with the size of 20 mm in 20 mm and thickness of 2 mm were obtained from Mazandaran Gas Company.

Synthesis of polyaniline

In the synthesis of PANI by polymerization, Aniline monomer and Ammonium peroxydisulfate were used in an acidic medium at room temperature. 0.2 M Aniline dissolved in 100 mL of 1 M HCl in a volumetric flask and also 0.5625 M APS was dissolved in 100 mL of 1 M HCl which added to the above solution dropwise for 2 hr. The mixture was stirred vigorously for 6. Next, the PANI precipitate was collected by filtration and repeatedly washed for 3 cycles with 1 M HCl and ethanol. The obtained powders were dried in an oven at 60 ° C for 24 hours [35].

Synthesis of doped polyaniline/alumina (PANI/Al_2O_3)

For doping of PANI, 0.2 M Aniline dissolved in 100 mL of 1 M HCl in a volumetric flask and 100 mg of Al_2O_3 was added to this solution. Then, 0.5625 M APS was dissolved in 100 mL of 1 M HCl which added to the above solution dropwise for 2 hr. The mixture was stirred vigorously for 6. Next, the precipitate was collected by filtration and repeatedly washed for 3 cycles with 1 M HCl and ethanol. The obtained powders were dried in an oven 24 hours at 60 ° C.

Preparation of coating color

In this part of the research, the obtained composite was added to the painting color in 3, 6, 9 and 12 percentages. Next, the steel sheets were colored by obtained coating color to be used in further experiments.

Preparation of PANI/Al_2O_3 composites coated steel

Steel coated with PANI/Al_2O_3 nanocomposite electrode with dimensions of 1 cm×1 cm was used to perform studies and investigate corrosion. In order to eliminate any impurities from the surface, acetone and trichlorethylene were applied for washing and cleaning. The PANI/Al_2O_3 nanocomposites were mixed by means of industrial paint formulations in different ratios by counting 3%, 6%, 9% and 12% by weight. In addition, an electrostatic spray gun was used to spray paint and nanocomposite on steel sheets with a thickness of 45 ± 3 μm. After uniform coating of paints and nanocomposites with different percentages was observed on steel sheets, the coated sheets were placed in an air-drying oven at 140 ° C for 20 minutes for baking. Coating bonds were evaluated using ASTM B117-19 salt spray test for each sample and it was found that it is able to provide analysis.

Characterization

FT-IR spectra of composite were recorded in the wavenumber varies between 400–4000 cm^{-1}. The thermal stability of samples was assessed by means of TGA instrument model STA 1500. The measurement was carried out in nitrogen atmosphere, in the temperature range, from 25-700 °C with heating rate of 10 °C/min. The morphology of the PANI and PANI/Al_2O_3 were evaluated by scanning electron microscopy (SEM, JSM-6700F). X-ray diffraction patterns were taken on a Micscience brand M18XHF diffractometer (MAC SCIENCE, Japan). All electrochemical measurements were performed on an AUTOLAB PGSTAT302N. Anti-corrosion studies of the PANI and PANI/Al_2O_3 color coated steel were performed in 3wt% NaCl solution by Electrochemical Impedance Spectroscopy (EIS), potentiodynamic polarization and open circuit potential methods. The paint coating thickness was measured by coating thickness gauge Wintact model WT2100. Moreover, salt spray test was done on the samples according to ASTMB117 standard.

RESULTS AND DISCUSSION

FT-IR Analysis

The FT-IR spectrum has been used to study the functional groups of polymers and the resulting polymer nanocomposites. Spectra were collected with a spectrometer using KBr pellets. The ratio of the sample to KBr was 1:100. In each case 1 mg of dried sample and 100 mg of KBr are homogenized using mortar and pestle thereafter pressed into a transparent tablet at 200 kgf/cm^2 for 5 min. The pellets are analyzed with a FT-IR spectrometer in the transmittance (%) mode with a scan resolution of 4 cm^{-1} and 64 scans by spectrum, over the 400–4000 cm^{-1} region. Fig. 1 shows the FT-IR spectrum of pure polyaniline, Al_2O_3 and PANI/Al_2O_3 nanocomposite. As shown in the Fig., the PANI absorption spectrum doped with hydrochloric acid (HCl) has specific bands in the range of 800-1600 cm^{-1}. According to the Fig., the bands in 1581 cm^{-1} and 1496 cm^{-1} are related to the tensile vibrations of quinonoid rings (N=Q=N) and benzonoid (N-B-N), respectively, and in fact indicate the conductivity of the polymer. The bands in 1384 cm^{-1} and 1265 cm^{-1} are also attributed to the N-H flexural vibration and the asymmetric C-N tensile vibration of the polaron PANI structure of the benzonoid ring. A clear and wide absorption band of about 1141 cm^{-1} is related to the C-N tensile vibration of the quinoid ring and indicates that no load is placed throughout the polymer structure. The band in the 802 cm^{-1} region is related to the C-H flexural vibration outside

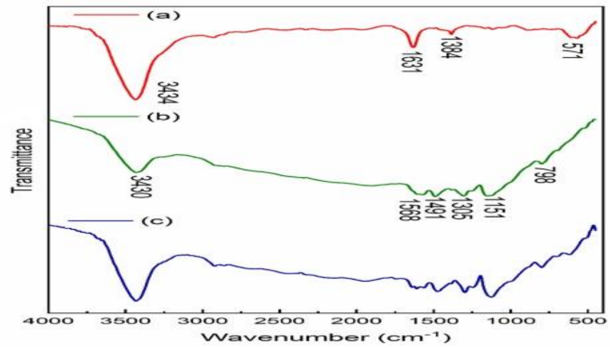

Fig. 1: FTIR spectra of (a) PANI (b), Al_2O_3 and (c) PANI -Al_2O_3

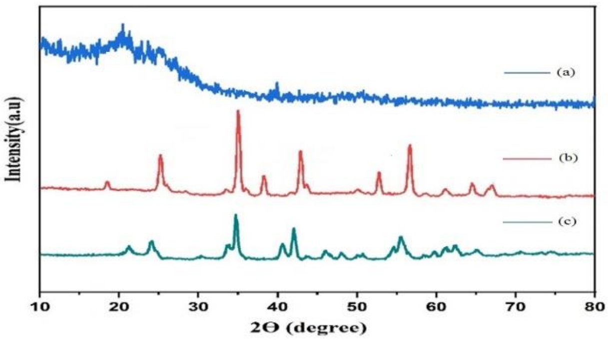

Fig. 2: XRD spectra of (a) PANI (b), Al_2O_3 and (c) PANI -Al_2O_3

the benzene ring

plate, and the wide band in the 3434 cm^{-1} range is also attributed to the N-H tensile vibration. The peak take shape at 613 cm^{-1} in the FT-IR spectrum of Al_2O_3 [Fig. 1(a)] was allocated to Al-O stretching vibration and the peak increases around 3430 cm^{-1} was attributed to O-H vibration form[36]. The O-H stretching of Al_2O_3 is revealed at 3490 cm^{-1}. The C=C stretching form of quinoid rings appear about 1568 cm^{-1} and 1491 cm^{-1}. The Al-O stretching appear at 508 cm^{-1}[37]. The mentioned outcomes results indicate that the PANI has been coated on the surface of Al_2O_3.

XRD analysis

The X-Ray Diffraction (XRD) curves of PANI, Al_2O_3 and PANI/Al_2O_3 nanocomposites can be seen in Fig. 2. As can be seen in the XRD pattern of the nanostructures (Fig. 2 (b)), the location of the peaks along with the intensities (2θ values = 26.52°, 35.74°, 39.30°, 44.50°, 53.26°, 57.46°, 66.26°, 68.31°) confirmed the formation of crystalline Al_2O_3 nanoparticles. Moreover, the XRD pattern of pure Al_2O_3 nanocrystal is compatible with that reported in the literatures [38, 39]. All Al_2O_3 peaks are present in the nanocomposite as shown in Fig. 2 (c), which indicates the precise synthesis of the nanocomposite. However, in the case of nanocomposites, there is little displacement in the position of the strips, which may be due to the interaction between polyaniline and Al_2O_3 nanoparticles, which leads to changes in the arrangement and formation of the polymer chains. The sharp and most intense peak of the XRD pattern was used to determine the crystalline particle size via Scherer equation (Eq. (1)).

$$D = \frac{K\lambda}{\beta \cos\theta} \quad (1)$$

In which, D is the crystalline particle size, β is the peak width at half maximum height (FWHM), λ is the wavelength of XRD radiation (1.54 Å), and θ is the diffraction position. Based on these obtained values, the crystallite size of 92 nm nanocomposite was obtained by Scherrer formula.

SEM Analysis

SEM analysis was used for investigating the shape, uniformity, and physical properties of the surface of the synthesized units, which are illustrated in Fig. 3. According to Fig. 3 (c), the structure of Al_2O_3 is in the form of fine clay particles. The structure of PANI/Al_2O_3 nanocomposite has the same structure as PANI itself due to the lower use of Al_2O_3 in the synthesis of nanocomposite compared to PANI. Another reason for this structure could be the complexation of Al_2O_3 by PANI to be converted to PANI crystalline nucleus in the synthesis method. This conclusion is consistent with the XRD curves. The formation of PANI coating on Al_2O_3 particles also increased the shell-core structure formation of nanoparticles.

Thermal properties

Fig. 4 illustrates thermo gravimetric analysis of PANI, Al_2O_3 and PANI- Al_2O_3. As can be seen, Al_2O_3 indicate elevated thermal stability and its property yield is around 90% at 600 ºC [40]. In the study of PANI, The TGA curve show three weight loss steps. The first one shows about 7 wt% weight losses under 100◦C, which can be assigned to the physically absorbed water evaporation. The second step corresponds to the polymer chain decomposition. The final steps (above 550ºC) also assigned to the perfect degradation of PANI. On the other hand, however, in study of PANI/Al_2O_3 nanocomposite, the main weight loss

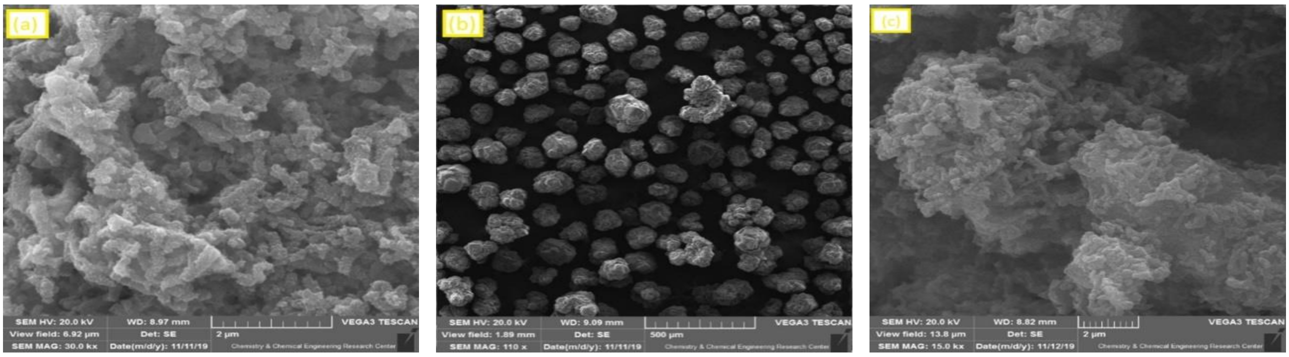

Fig. 3: *SEM spectra of (a) PANI (b) Al_2O_3 (c) PANI- Al_2O_3*

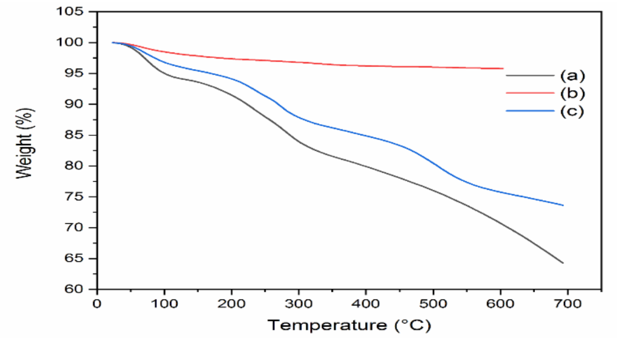

Fig.. 4: *TGA spectra of (a) PANI (b) Al_2O_3 (c) PANI- Al_2O_3*

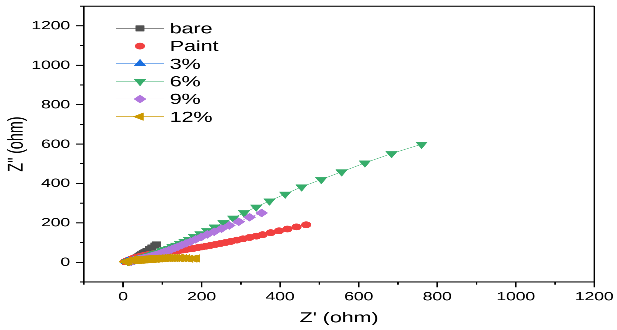

Fig. 5: *Nyquist plots of (a) bare steel, (b)coating paint, (c) PANI- Al_2O_3 3%wt, (d) PANI- Al_2O_3 6%wt, (e) PANI- Al_2O_3 9%wt and (f) PANI- Al_2O_3 12%wt, as a function of time in 3 % sodium chloride solution*

decrease was observed at lower temperature and above 340 ^{0}C. According to the TGA curves, Al_2O_3 indicate elevated thermal stability and its property yield is around 90% at 600 ºC [40]. the thermal stability PANI- Al_2O_3 is in between Al_2O_3 and PANI, which emphasizes the doping of Al_2O_3 to PANI.

EIS analysis of PANI/Al_2O_3 -containing coating

The EIS method is a powerful tool for analyzing and studying corrosion and adsorption phenomena. EIS measurements are performed to obtain information about

Table 1: *The corrosion potentials and corrosion current of bare steel, PANI/Al2O3 -containing coating and paint coating in 3.5 wt% NaCl solution*

Sample	E_{corr}	i_{corr} (A/cm^{-2})
Bare Steel	-0.4705	0.0086
Steel coated paint	-0.5888	0.0083
PANI- Al_2O_3 3% wt	-0.6790	0.0027
PANI- Al_2O_3 6% wt	-0.6683	0.0018
PANI- Al_2O_3 9% wt	-0.6625	0.0029
PANI- Al_2O_3 12% wt	-0.6373	0.0021

the inhibition processes. The Nyquist curve represents a capacitive ring that deviates from an ideal semicircle. The diameter of the semicircle is approximately equal to the amount of charge transfer resistance of the corrosion reaction process. Fig. 5 shows the Nyquist diagram of the uncoated electrode and the PANI/Al_2O_3 nanocomposite electrode with different weight percentages. According to the Fig., the current transfer resistance increases with increasing amount of nanocomposite, so that it increases by up to 6% by weight and decreases for larger amounts. The current transfer resistance increases from 100 ohms to 890 ohms for the optimal amount of suspension relative to the uncoated electrode and decreases for later values. As a result, it can be seen that PANI/Al_2O_3 nanocomposite of 6 wt% has the highest resistance [41].

Polarization curve analysis

Fig. 6 shows the Tafel plot of PANI/Al_2O_3 nanocomposite with different weight percentages, and Table 1 shows the related parameters. As shown in the Fig. 6, a corresponds to the uncoated electrode, b corresponds to the industrial paint coated electrode, and c-f corresponds to the electrodes coated with PANI/Al_2O_3 nanocomposite weight percentage of 3, 6, 9, 12 wt%, respectively.

Table 2: Comparison between the studies about PANI containing various fillers in enhancing the corrosion resistance of coatings

Sample	E_{corr}	i_{corr} (A cm^{-2})	Reference
CaCO3–PANI	-1.47	0.003	[43]
PANI/Zn/Ce$(NO_3)_3$	-0.572	0.0037	[44]
PANI-$FeCl_2$/H_2O_2	-0.542	0.0016	[45]
SiO_2@polyaniline	-0.512	0.0012	[46]
PPY-Al_2O_3	-0.6625	0.0029	[47]
Polyaniline-Boron nitride-PVA	-0.44	0.00103	[48]
This work	-0.6373	0.0018	--

Table 3: OCP amounts with different composition in paint coating

Sample	OCP
Coating paint	- 0.6950
PANI- Al_2O_3 3% wt	- 0.5740
PANI- Al_2O_3 6% wt	-0.5668
PANI- Al_2O_3 9% wt	- 0.6210
PANI- Al_2O_3 12% wt	- 0.6620

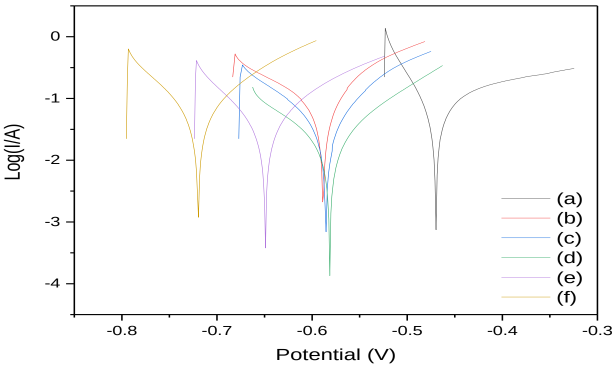

***Fig. 6:** Polarization curves of (a) bare steel, (b)coating paint, (c) PANI- Al_2O_3 3%wt, (d) PANI- Al_2O_3 6%wt, (e) PANI- Al_2O_3 9%wt and (f) PANI- Al_2O_3 12%wt, in 3.5 % sodium chloride solution*

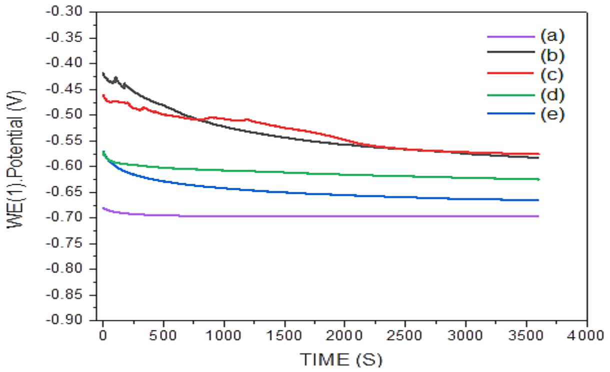

***Fig. 7:** Open circuit potential of (a) coating paint (b) PANI- Al_2O_3 3%wt, (c) PANI- Al_2O_3 6%wt, (d) PANI- Al_2O_3 9%wt and (e) PANI- Al_2O_3 12%wt, as a function of time in 3.5 % sodium chloride solution*

The Tafel test is used to check the corrosion current of metal surfaces in a corrosive environment. The values of Ecorr (corrosion potential) and Icorr (corrosion current) obtained from extrapolation of Tafel plot. The Icorr represents the intensity of cathodic reduction of oxygen and anodic dissolution of metal ions and a lower value of Icorr represents a lower corrosion dynamic rate In Fig. 6, the corrosion current of the nanocomposites were lower than the other samples, and the PANI/Al_2O_3 6%wt curve was lower than the PANI- Al_2O_3 9%wt and PANI/Al_2O_3 12%wt, indicating a higher anticorrosion resistance. According to the Tafel curves, nanocomposite coatings containing PANI/Al_2O_3 6%wt was decisively superior to other coatings. The corrosion current of the composite contains PANI/Al_2O_3 6%wt equal to 0.0018 mA cm^{-2}, which is the lowest corrosion current among all samples. Then, PANI- Al2O3 12%wt and PANI- Al2O3 3%wt composites have currents of 0.0021 and 0.0027 mA cm^{-2}, respectively. Also, according to the intersection points of the anodic and cathodic slopes, the curve of the amount of current and potential of each was obtained, and is illustrated in Table 1. Compared with other studies, according to the corrosion current density, prepared coating in this study has a good barrier effect on corrosion of mild steel. [42].

Also, the comparison between the results of Tafel analysis of this research with other similar researches is shown in Table 2.

Open circuit potential analysis

The purpose of the Open Circuit Potential (OCP) test is to evaluate the amount of corrosion potential of metals. In OCP test, the higher the corrosion potential causes the better the corrosion resistance of the coating. In Fig. 7, the synthesized nanocomposites have a higher corrosion potential than the other samples. It was also observed that the corrosion potential of PANI/Al_2O_3 6%wt composites coating was higher than the corrosion potential of other

Table 4: Salt spray test in 24 and 48h

Sample	Amount Corrosion % (24h)	Amount Corrosion % (48h)
Bare steel	90	100
Steel coated paint	10	70
PANI- Al_2O_3 6% wt	1-2	10

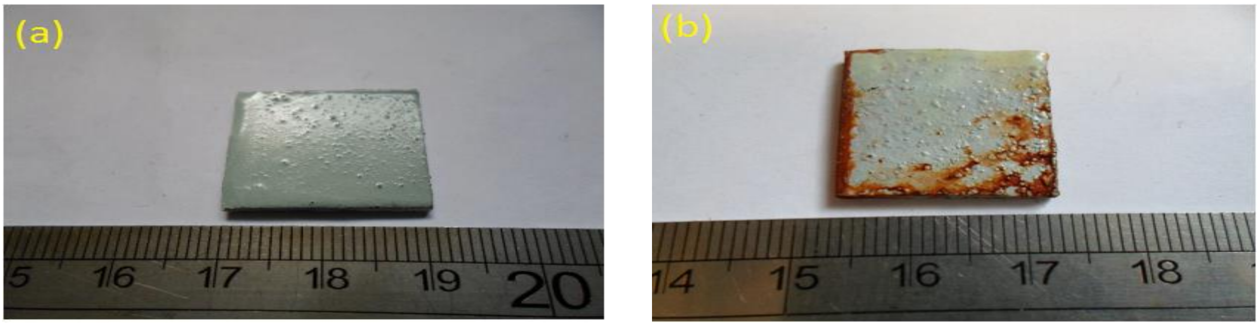

Fig.8: (a) Before and (b) after the Salt spray test

coating. As can be seen in Fig. 7, after a small increase in ocp at the first steps of time, the OCP remained relatively constant after 2000 s which could be ascribed to the passivation of the surfaces.

Salt spray test

The salt spray test is a standardized and popular corrosion test method, used to check corrosion resistance of materials and surface coatings. In this study, the salt spray test was carried out on the coatings by artificial scribe to show the active inhibiting part of PANI/Al_2O_3 particles in the coating as well. Based on to salt spray test outcome given in Fig. 8, the enhancement of exposure time caused to enhancement of coating delamination part at defect area, corrosion outcomes creation at and about the scribe on both pure paint and composite containing samples. The coating delamination and corrosion outcome procedure beneath the coating were generally pronounced for the pure paint system. Nevertheless, outcome evidently confirm that the coating filled by PANI/Al_2O_3 nanocomposite demonstrate no delamination and corrosion products improvement at and about scribe at all immersion period. This examination obviously exhibits the active inhibition task of PANI and Al_2O_3 particles in prevention of coating delamination as of defect area. Based on Table 4, the quantity of corrosion has declined from 100% to 10% afterward 48 hours, which indicates the effective attendance of the PANI/Al_2O_3 6%wt composite.

Anticorrosion mechanism of the PANI/Al_2O_3 containing coating

According to the results of electrochemical testing, it can be inferred that the coating containing PANI/Al_2O_3 nanocomposite has a significant anodic protective effect, which is associated with a change in the positive potential region, reduced corrosion current and a tendency to resist. The anodic defense of the coating containing PANI/Al_2O_3 nanocomposite is limited by the anode reaction method. The cathodic reaction load by PANI/Al_2O_3 nanocomposites can be transferred to the coating surface. PANI/Al_2O_3 nanocomposite plays an important role in the anti-corrosion properties of steel in industrial coatings. Protection, deterrence and anodic protection are the main protective function of the coating containing PANI/Al_2O_3 nanocomposite with paint.

CONCLUSIONS

In this paper, PANI/Al_2O_3 nanocomposite was prepared by chemical oxidative polymerization method and the anti-corrosion ability of nanocomposite was investigated as pigment blend with commercial paint. Synthesized nanocomposites were characterized using FT-IR, XRD, TGA and SEM. The anticorrosion capability of the product was measured using the entirely immersion analyze sodium chloride solution according to ASTM B117-19 standard method. Results indicated that, coatings containing PANI/Al_2O_3 nanocomposite with paint have a higher impact potential than the coating of pure paint in 3.0% NaCl solution. The reason for the good protective performance of the coating containing PANI/Al_2O_3 along with the paint is due to its anodic control and protection. Also, the anticorrosion ability of coating containing 6 % PANI/Al_2O3 along with the paint is more than other samples in 3 % NaCl solution.

Received : Dec. 21, 2022 ; Accepted : Apr. 23, 2023

REFERENCES

[1] Sepeur S., Goedicke S., Reuter N., Coating Material for Protecting Metals, Especially Steel, From Corrosion and/or Scaling, Method for Coating Metals and Metal Element. 2010, Google Patents.

[2] Kusmierek E., Chrzescijanska E., Atmospheric Corrosion of Metals in Industrial city Environment, *Data Brief*., **3**: 149-154 (2015).

[3] Badilla G. L., salas B., Zlatev R., Flores J. F., Corrosion of Metals at Indoor Conditions in the Electronics Manufacturing Industry, *Anti-Corros Methodes M*., **54**: 354-359 (2007).

[4] Kaesche H., Corrosion of Metals: Physicochemical Principles and Current Problems, 2003, pringer Science & Business Media.

[5] Frankel G. Errata S., Pitting Corrosion of Metals. A Review of the Critical Factors, *J. Electrochem. Soc.*, **145**: 2186-2198 (1998).

[6] Giggins C.S., Pettit F.S., Corrosion of Metals and Alloys in Mixed Gas Environments at Elevated Temperatures, *Oxid. Met*., **14**: 363-413 (1980).

[7] López D.A., Pérez T., The influence of Microstructure and Chemical Composition of Carbon and Low Alloy Steels in CO_2 Corrosion. A State-of-the-Art Appraisal, *Mater. Des*., **24**: 561-575 (2003).

[8] Jaqanathan B., Matur G., Corrosion Protection of Copper with Hybrid Sol-Gel Containing 1H-1, 2, 4-triazole-3-thiol, *Iran. J. Chem. Chem. Eng. (IJCCE)* **4**: 61-71 (2016).

[9] Schweitzer P.A., "Fundamentals of Metallic Corrosion: Atmospheric and Media Corrosion of Metals", CRC Press (2006).

[10] Soares C.G., Garbatov Y., Zayed A., Effect of Environmental Factors on Steel Plate Corrosion under Marine Immersion Conditions, *Corros. Eng. Sci. Technol*., **46**: 524 (2011).

[11] Elmi S., Foroughi M. M., Dehdab M., Shahidi-Zandi M., Computational Evaluation of Corrosion Inhibition of Four Quinoline Derivatives on Carbon Steel in Aqueous Phase, *Iran. J. Chem. Chem. Eng. (IJCCE)*, **38**: 185-200 (2019).

[12] Daniyal M., Akhtar S., Corrosion Assessment and Control Techniques for Reinforced concrete Structures: A Review, *Journal of Building Pathology and Rehabilitation*., **5**: 1-12 (2019).

[13] Weck P.F., Jové-Colón C.F., Kim E., Thermodynamic Properties of Metaschoepite Predicted from Density Functional Perturbation Theory, *Chem. Phys. Lett.*, **757**: 137878 (2020).

[14] Farzaneh A., Jaber N., Jamshid M., An Electrochemical Measurement for Evaluating the Cathodic Disbondment of Buried Pipeline Coatings under Cathodic Protection, *Iran. J. Chem. Chem. Eng. (IJCCE)* **34**: 83-91 (2015).

[15] Altaf F., Qureshi R., Yaqub A., Ahmed S., Electrochemistry of Corrosion Mitigation of Brasses by Azoles in Basic Medium, *Chem. Pap*., **73**: 1221-1235 (2019).

[16] Stejskal J., Conducting Polymers are Not Just Conducting: A Perspective for Emerging Technology, *Polym. Int*., **69**: 662-664 (2020).

[17] Qian Y., Li Y., Jungwirth S., Seely N., The Application of Anti-Corrosion Coating for Preserving the Value of Equipment Asset in Chloride-Laden Environments: A, *Int. J. Electrochem. Sci*., **10**: 10756-10780 (2015).

[18] Yaser J., Ghoreishi S.M., Shabani M., Electrosynthesis, Characterization and Corrosion Inhibition Study of DBSA-doped Polyaniline Coating on 310 Stainless Steel, *Iran. J. Chem. Chem. Eng. (IJCCE)*, **36**: 23-32 (2017).

[19] Gangopadhyay R., Amitabha D., Conducting Polymer Nanocomposites: A Brief Overview, *Chem. Mater*., **12**: 608-622 (2000).

[20] C. I. Awuzie, Conducting Polymers, Materials Today: Proceedings., **4**: 5721-5726 (2017)

[21] Ozkan B.C., Soganci T., Turhan H., Ak M., Investigation of rGO and Chitosan Effects on Optical and Electrical Properties of the Conductive Polymers for Advanced Applications, *Electrochim. Acta.,* **295**: 1044-1051 (2019).

[22] Balint R., Cassidy N.J., Cartmell S.H., Conductive Polymers: Towards a Smart Biomaterial for Tissue Engineering, *Acta Biomater.*, **10**: 2341-2353 (2014).

[23] Wu X., Markir A., Xu Y., Zhang C., Leonard D.P., Shin W., Ji X., A Low-Cost and Dendrite-Free Rechargeable Aluminium-Ion Battery with Superior Performance, *Adv. Electron. Mater.*, **29**: 1900911 (2019).

[24] Moshayedi H.R., Rabiee, M., Rabiee, N., Graphene Oxide/Polyaniline-Based Multi Nano Sensor for Simultaneous Detection of Carbon Dioxide, Methane, Ethanol and Ammonia Gases, *Iran. J. Chem. Chem. Eng. (IJCCE)*, **39(3)**: 55-64 (2020).

[25] AlSalhi M. S., Alam J., Dass L. A., Raja M., Recent Advances in Conjugated Polymers for Light Emitting Devices, *Int. J. Mol. Sci.*, **12**: 2036-2054 (2011).

[26] Bhadra S., Khastgir D., Singha N., Lee J.H., Progress in Preparation, Processing and Applications of Polyaniline, *Prog. Polym. Sci.*, **34**: 783-810 (2009).

[27] Roy W., Saxena S. K., Yogi P., Pathak D. K., Chaudhary A., Kumar R., Structural and Optical Properties of Polyaniline-Green Silver Nanocomposite, *J. Mater. Process. Technol.*, **5**: 172-180 (2019).

[28] Wahid U., Hajera G., Rizwan U., Salma G., Anwar A. S., Salma B., Corrosion Inhibition Properties of Sulfonated Polyaniline-Poly(Vinyl Alcohol) Composite on Mild Steel, *Iran. J. Chem. Chem. Eng. (IJCCE)*, **21(4):** 1313-1321 (2022).

[29] Pour-Ali S., , Dehghanian C., Kosari A., Corrosion Protection of the Reinforcing Steels in Chloride-Laden Concrete Environment Through Epoxy/Polyaniline–Camphorsulfonate Nanocomposite Coating, *Corros. Sci.*, **90**: 39-247 (2015).

[30] Saravanan R. , Sacari E., Gracia F., M. Khan M., Mosquera E., Gupta V.K., Conducting PANI Stimulated ZnO System for Visible Light Photocatalytic Degradation of Coloured Dyes, *J. Mol. Liq.*, **221**: 1029-1033 (2016).

[31] Li J., Zhu L., Wu Y., Harima Y., Hybrid Composites of Conductive Polyaniline and Nanocrystalline Titanium Oxide Prepared via Self-Assembling and Graft Polymerization, *Polymer*., **47**: 7361-7367 (2006).

[32] Gupta V., Miura N., Polyaniline/Single-Wall Carbon nanotube (PANI/SWCNT) Composites for High Performance Supercapacitors, *Electrochim. Acta*., **52**: 1721-1726 (2006).

[33] Yue S., Ji W., Liu C., Xu J., Synergistic Effect of Homogeneously Dispersed PANI-TiN Nanocomposites Towards Long-Term Anticorrosive Performance of Epoxy Coatings, *Prog. Org. Coat*., **130**: 156-167 (2019).

[34] Park O., Jeevananda T., Kim N. H., Kim S., Photovoltaic Characteristics of Multiwalled Carbon Nanotube Counter-Electrode Materials for Dye-Sensitized Solar Cells Produced by Chemical Treatment and Addition of Dispersant, *Scr. Mater*., **9**: 250-262 (2019).

[35] Ghasemi A.K., Ghorbani M., Lashkenari M.S., Nasiri N., Facile Synthesize of PANI/GO/$CuFe_2O_4$ Nanocomposite Material with Synergistic Effect for Superb Performance Supercapacitor, *Electrochimica Acta***, 439**: 141685 (2023).

[36] Zaki M. I., Hasan M. A., Al-Sagheer F., Pasupulety L., In situ FTIR Spectra of Pyridine Adsorbed on SiO_2–Al2O_3, TiO_2, ZrO_2 and CeO_2: General Considerations for the Identification of Acid Sites on Surfaces of Finely Divided Metal Oxides, *Colloids Surf. A Physicochem. Eng. Asp.*, **190**: 261-274 (2001).

[37] Djebaili K., Mekhalif Z., Boumaza A., Djelloul A., XPS, FTIR, EDX, and XRD Analysis of Al_2O_3 Scales Grown on PM2000 Alloy, *Int. J. Spectrosc*., **868109**: 1-16 (2015)

[38] Sui X., Chu Y., Xing S., Liu C., Synthesis of PANI/AgCl, PANI/$BaSO_4$ and PANI/TiO_2 Nanocomposites in CTAB/Hexanol/Water Reverse Micelle, *Mater. Lett*., **58**: 1255-1259 (2004).

[39] Sanches E.A., Soares J.C., Mafud A.C., Fernandes E.G.R., Leite F.L., Mascarenhas Y.P., Structural Characterization of Chloride Salt of Conducting Polyaniline Obtained by XRD, SAXD, SAXS and SEM, J. Mol. Struct., **1036**: 121-126 (2013).

[40] Zhu J., Wei S., Zhang L., Mao Y., Ryu J., Haldolarchige N., Young D. P., Guo Z., Electrical and Dielectric Properties of Polyaniline–Al_2O_3 Nanocomposites Derived from Various Al_2O_3 Nanostructures, J. Mater. Chem., **21**: 3952-3959 (2011).

[41] Ghasemi A.K., Ghorbani M., Lashkenari M.S., Nasiri N., Controllable Synthesis of Zinc ferrite Nanostructure with Tunable Morphology on Polyaniline Nanocomposite for Supercapacitor Application, *Journal of Energy Storage*, **51**: 104579 (2022).

[42] Lei Y., Qiu Z., Tan N., Du H., Li D., Liu J., Liu Tao, Zhang W., Chang X., Polyaniline/CeO_2 Nanocomposites as Corrosion Inhibitors for Improving the Corrosive Performance of Epoxy Coating on Carbon Steel in 3.5% NaCl Solution, *Prog. Org. Coat*., **139** :105430 (2020).

[43] Bhanvase B.A., Sonawane S.H., New Approach for Simultaneous Enhancement of Anticorrosive and Mechanical Properties of Coatings: Application of Water Repellent Nano $CaCO_3$–PANI Emulsion Nanocomposite in Alkyd Resin, *Chem. Eng. J*., **156**: 177-183 (2010).

[44] Li Z., Hu J., Li Y., Liu J., Renewable Protein-Based Monomer for Thermosets: A Case Study on Phthalonitrile Resin, *React. Funct. Polym*., **20** :5158-5168 (2018).

[45] Hou W.P., Liu Y., Ge Z.Y., Zhao W.Y., Recent Progress in the Preparation of Polyaniline Nanostructures and Their Applications in Anticorrosive Coatings, *Mater. Corros.*, **4**: 28195-28208 (2014).

[46] Weng C.-J., Chen Y.-L., Jhuo Y.-S., Yi-Li L., Yeh J.M., Advanced Antistatic/Anticorrosion Coatings Prepared from Polystyrene Composites Incorporating Dodecylbenzenesulfonic Acid-Doped SiO_2@Polyaniline Core–Shell Microspheres, *Polym. Int.*, **62**: 774-782 (2013).

[47] Ehsani A., Mahjani M.G., Nasseri M., Jafarian M., Influence of Electrosynthesis Conditions and Al_2O_3 Nanoparticles on Corrosion Protection Effect of Polypyrrole Films, *Anti-Corros Method M.*, **3**: 146-152 (2014).

[48] Sarkar N., Sahoo G., Das R., Prusty G., Sahu D., Swain S.K., Anticorrosion Performance of three-Dimensional Hierarchical PANI@ BN Nanohybrid, *Industrial & Engineering Chemistry Research*, **55**: 2921-2931(2016).